NOAA Technical Memorandum OAR-PMEL-146

MOORED ACOUSTIC DOPPLER CURRENT PROFILER TIME SERIES IN THE CENTRAL EQUATORIAL INDIAN OCEAN

Y. Wang[1], M. J. McPhaden[2], P. Freitag[2], and C. Fey [2,3]

1 College of Physical and Environmental Oceanography, Ocean University of China, Qingdao, Shandong, China
2 NOAA Pacific Marine Environmental Laboratory, Seattle, WA
3 Joint Institute for the Study of Atmosphere and Ocean (JISAO), University of Washington, Seattle, WA

April 2015

UNITED STATES DEPARTMENT OF COMMERCE

Penny Pritzker
Secretary

NATIONAL OCEANIC AND ATMOSPHERIC ADMINISTRATION

Kathy Sullivan
Under Secretary for Oceans and Atmosphere/Administrator

Office of Oceanic and Atmospheric Research

Craig McLean
Assistant Administrator

NOTICE from NOAA

Mention of a commercial company or product does not constitute an endorsement by NOAA/ OAR. Use of information from this publication concerning proprietary products or the tests of such products for publicity or advertising purposes is not authorized. Any opinions, findings, and conclusions or recommendations expressed in this material are those of the authors and do not necessarily reflect the views of the National Oceanic and Atmospheric Administration.

Contribution No. 4307 from NOAA/Pacific Marine Environmental Laboratory

Contribution No. 2427 from Joint Institute for the Study of the Atmosphere and Ocean (JISAO)

Also available from the National Technical Information Service (NTIS)

(http://www.ntis.gov)

Contents

List of Figures

List of Tables

Moored acoustic Doppler current profiler time series in the central equatorial Indian Ocean

Y. Wang[1], M. J. McPhaden[2], P. Freitag[2], and C. Fey[2,3]

Abstract. This report summarizes the processing of moored acoustic Doppler current profiler (ADCP) data from several locations centered at 0°, 80.5°E for the period August 2008 to August 2012. Sampling, gridding, filtering, and gap filling are described. Original and processed time series data are presented for records at each site.

1. Introduction

Ocean current has been measured in the vicinity of 0°, 80.5°E since August 2008 from an array of upward looking acoustic Doppler current profilers (ADCPs) within the Research Moored Array for African-Asian-Australian Monsoon Analysis and Prediction (RAMA) program (McPhaden *et al.*, 2009). Eight sites are situated along an 80.5°E meridional section and two more sites are located on either side of 80.5°E on the equator (**Figure 1**). The 0°, 80.5°E mooring is common to both sections and is a permanent component of RAMA, with measurements beginning at that site in October 2004. The array of moorings is located in the central equatorial Indian Ocean where semi-annual eastward Wyrtki Jets are a prominent feature of the ocean circulation (Wyrtki, 1973) and where the anomalous easterly winds and currents are strongly associated with Indian Ocean Dipole (IOD) events (Saji *et al.*, 1999). Over four years of current profiler data (August 2008–August 2012) covering depths of 35 m to >200 m with 8 m vertical resolution are available from this array.

The purpose of this report is to summarize the processing of these mooring data. The analysis and application of the current data from 0°, 80.5°E measured during 2004–2008 have appeared previously in the literature (e.g., Masumoto *et al.*, 2008; Nagura and McPhaden, 2008, 2010a,b; Iskandar and McPhaden, 2011; Gnanaseelan *et al.*, 2012). This report considers processing of the data for the full array.

1 College of Physical and Environmental Oceanography, Ocean University of China, Qingdao, Shandong, China

2 NOAA Pacific Marine Environmental Laboratory, Seattle, WA

3 Joint Institute for the Study of Atmosphere and Ocean (JISAO), University of Washington, Seattle, WA

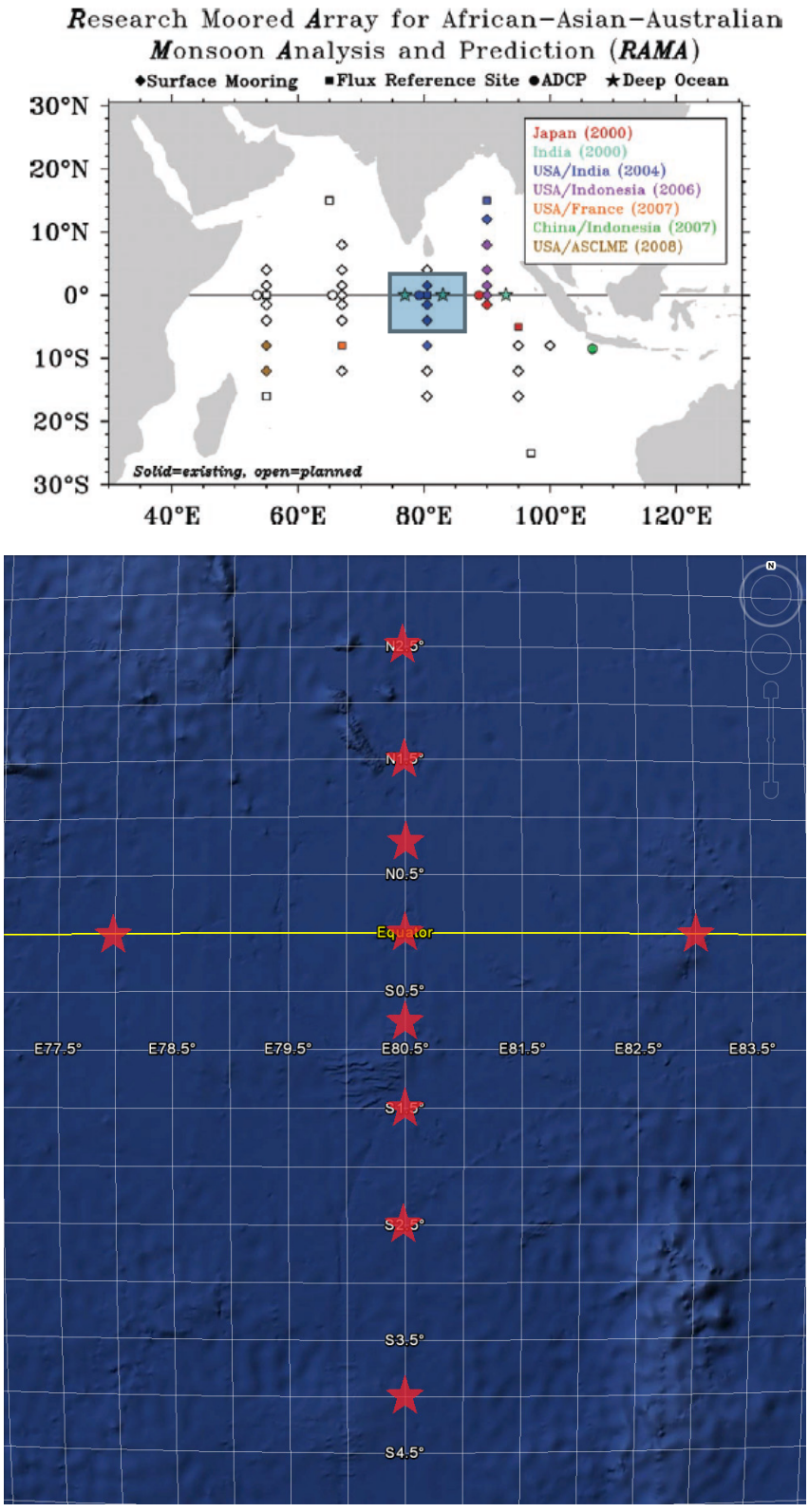

Figure 1. (Top:) The RAMA moored buoy array highlighting the region in blue shading where the ADCP array is situated. (Bottom:) Locations of the ADCP mooring sites nested in RAMA.

2. Background Information

The mooring data used in this study consist of horizontal currents from eight sites along 80.5°E (4°S, 2.5°S, 1.5°S, 0.75°S, 0.75°N, 1.5°N, and 2.5°N) and three sites along the equator (78°E, 80.5°E, and 83°E). The data were collected from subsurface moorings with ADCPs mounted in a float located at depths of about 300–400 m (**Figure 2**). Mooring deployments and recoveries were made at 6-month to 2-year intervals. Time series of the original data at each site are shown in **Figures 3** and **4**. The time series at 0°, 80.5°E spans October 2004 to August 2012, while at the other sites they span August 2008 to August 2012. Gaps in the time series are due to occasional instrument or mooring failures.

The current data were measured by upward looking 75 kHz RDI Longranger ADCPs. Hourly averaged horizontal-velocity components were recorded from ensembles of 40 pings at 90 s repetition rates at 8 m vertical resolution. Recorded velocity data are relative to the head depth, which is measured by a pressure sensor on the instrument, plus two additional pressure sensors on the buoy frame. Velocity data were gridded to 5 m resolution after adjustment of bin lengths based on speed of sound from historical CTDs near the mooring (Plimpton *et al.*, 2004). The observed range to the sea surface was also used in the gridding process.

Dates and the estimated depths of the ADCP head for each deployment are listed in **Table 1**. The moored ADCPs deployed in August 2011 at 2.5°N, 80.5°E, 2.5°S, 80.5°E, and 4.0°S, 80.5°E have not been recovered yet. Hence, the time series at these three sites only cover three years (August 2008 to August 2011) as of this writing.

The target depth for the ADCP heads in each deployment was 300 m, but the actual depth ranged between 257 and 455 m (**Table 1**). Thus, the time series of the currents deeper than 200 m were less often observed. In addition, the magnitude of the horizontal current velocity weakened with increasing depth. Therefore, we focused our processing on data at depths shallower than 200 m depth.

Velocity retrievals near the surface are contaminated by backscatter from the ocean surface. Hence, near-surface measurements were discarded in the upper 20–40 m. To evaluate various approaches of extrapolating the ADCP to the surface, we used Sontek current records at 10 m depth from three taut-line surface ATLAS moorings in close proximity to the ADCP moorings at 1.5°, 0°, and 1.5°N along 80.5°E.

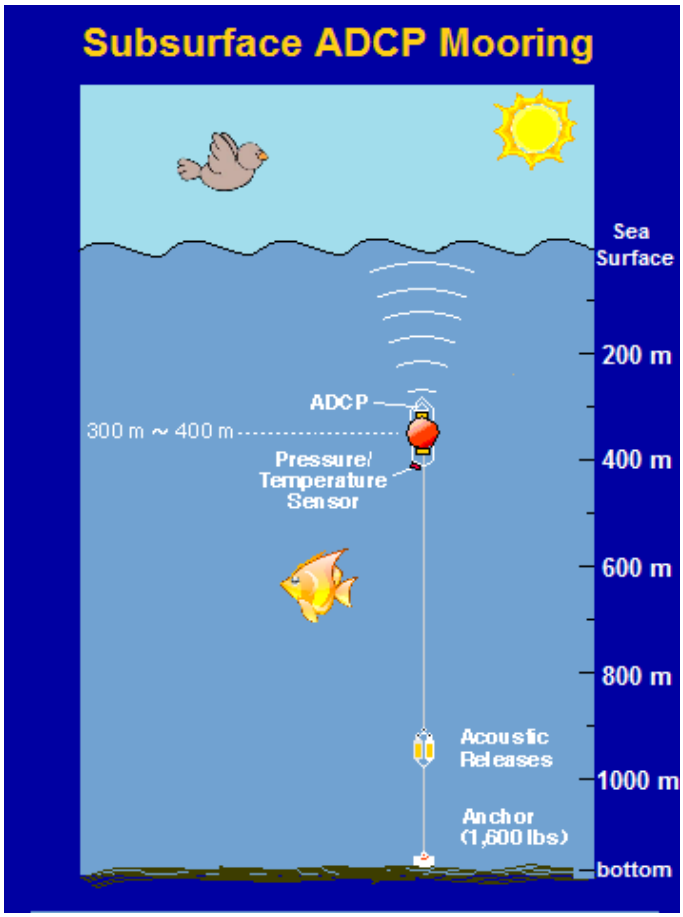

Figure 2: Schematic of a moored ADCP.

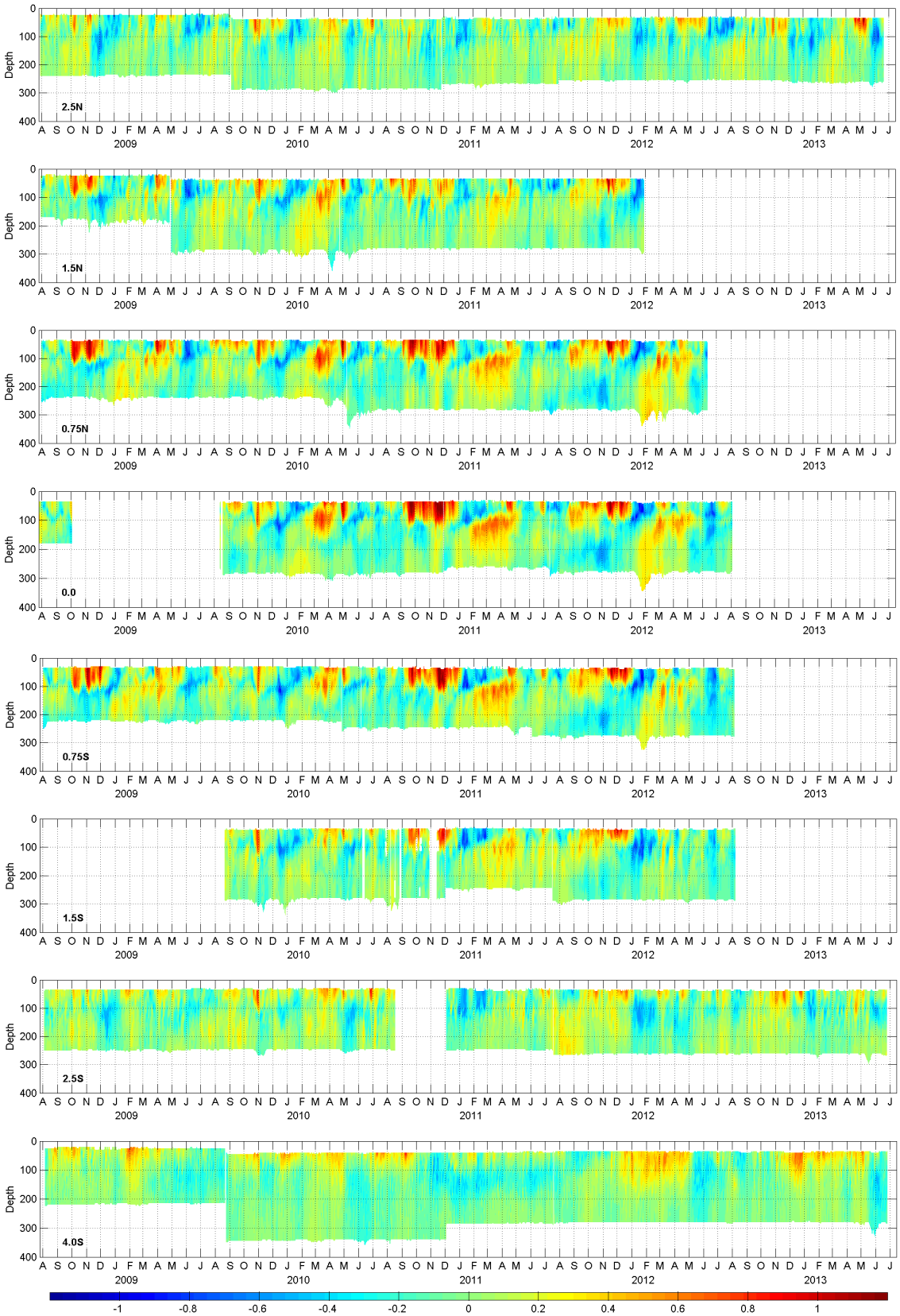

Figure 3a: The original dataset: Zonal velocity along the 80.5°E meridional section.

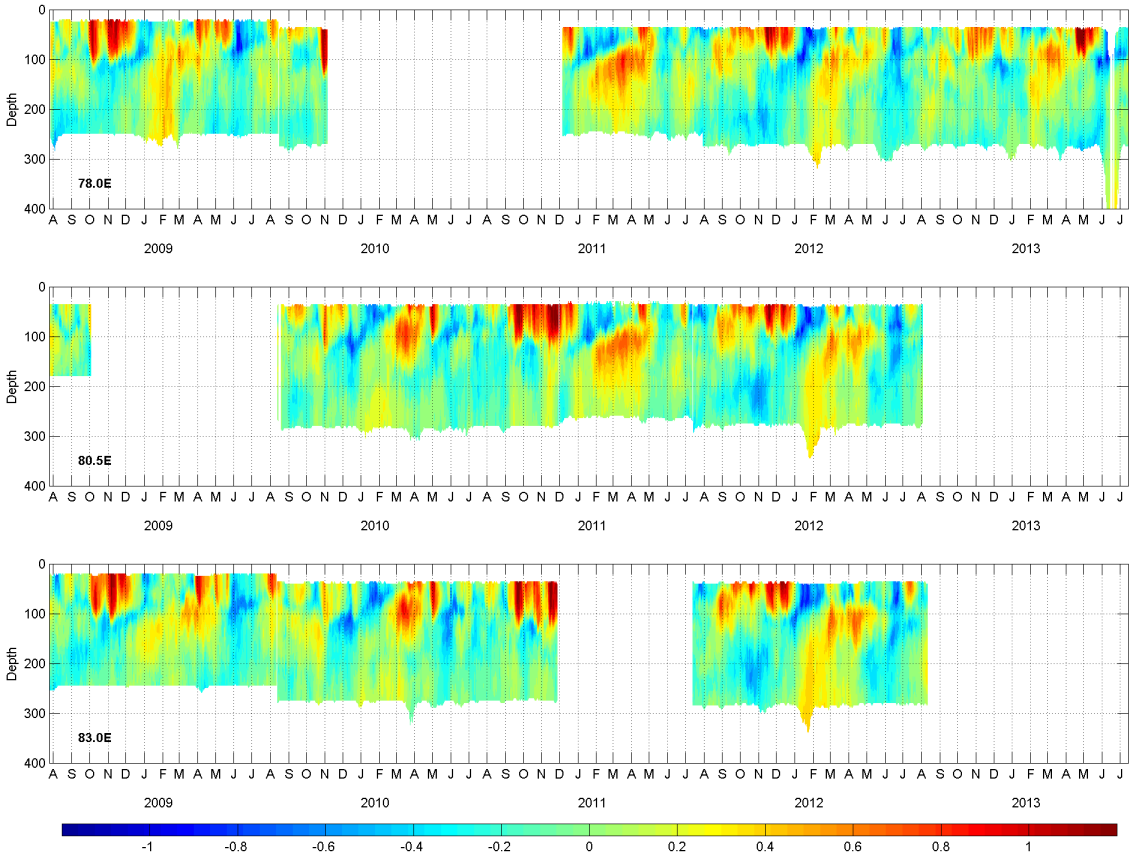

Figure 3b: The original dataset: Zonal velocity along the equator.

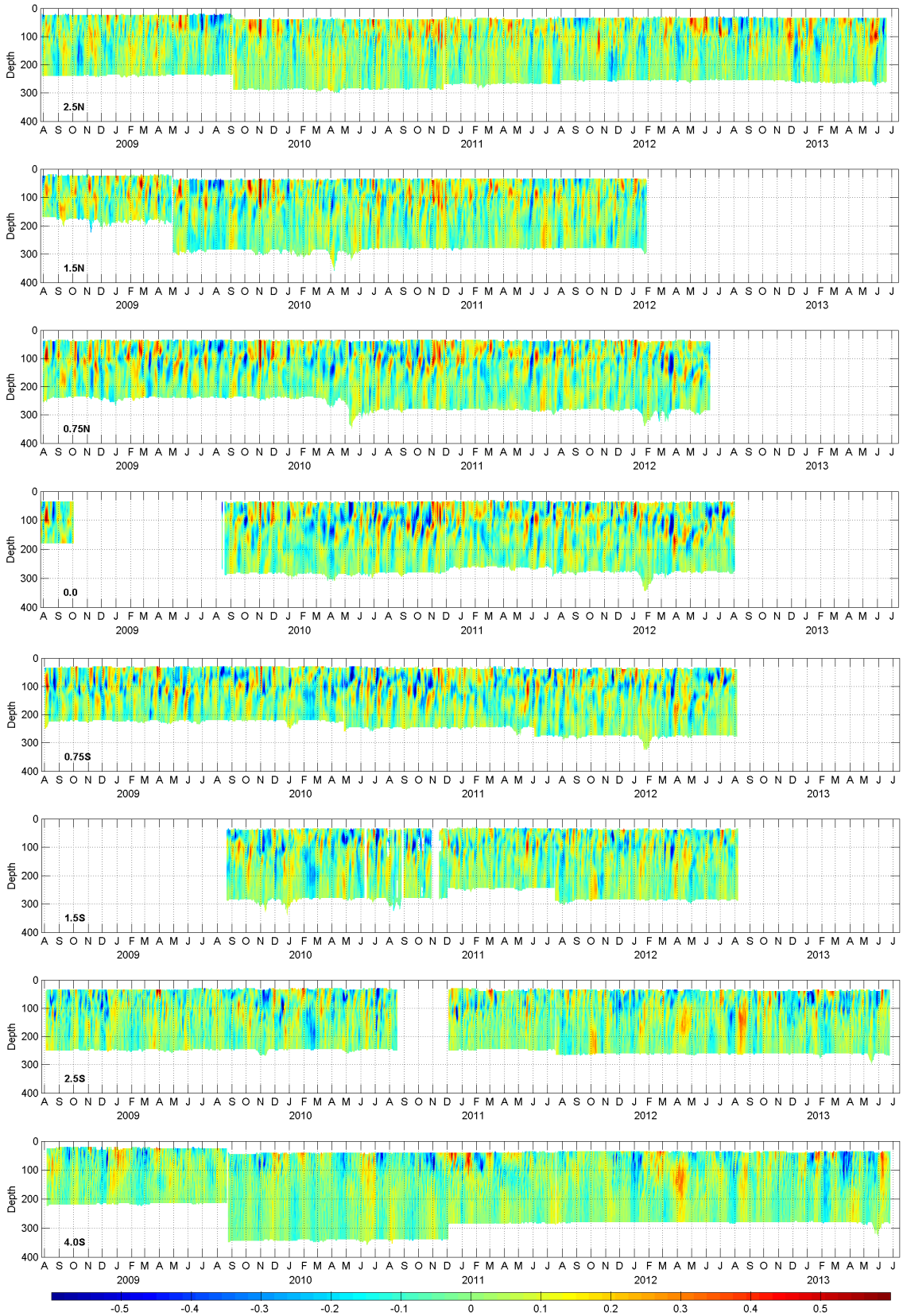

Figure 4a: The original dataset: Meridional velocity along the 80.5°E meridional section.

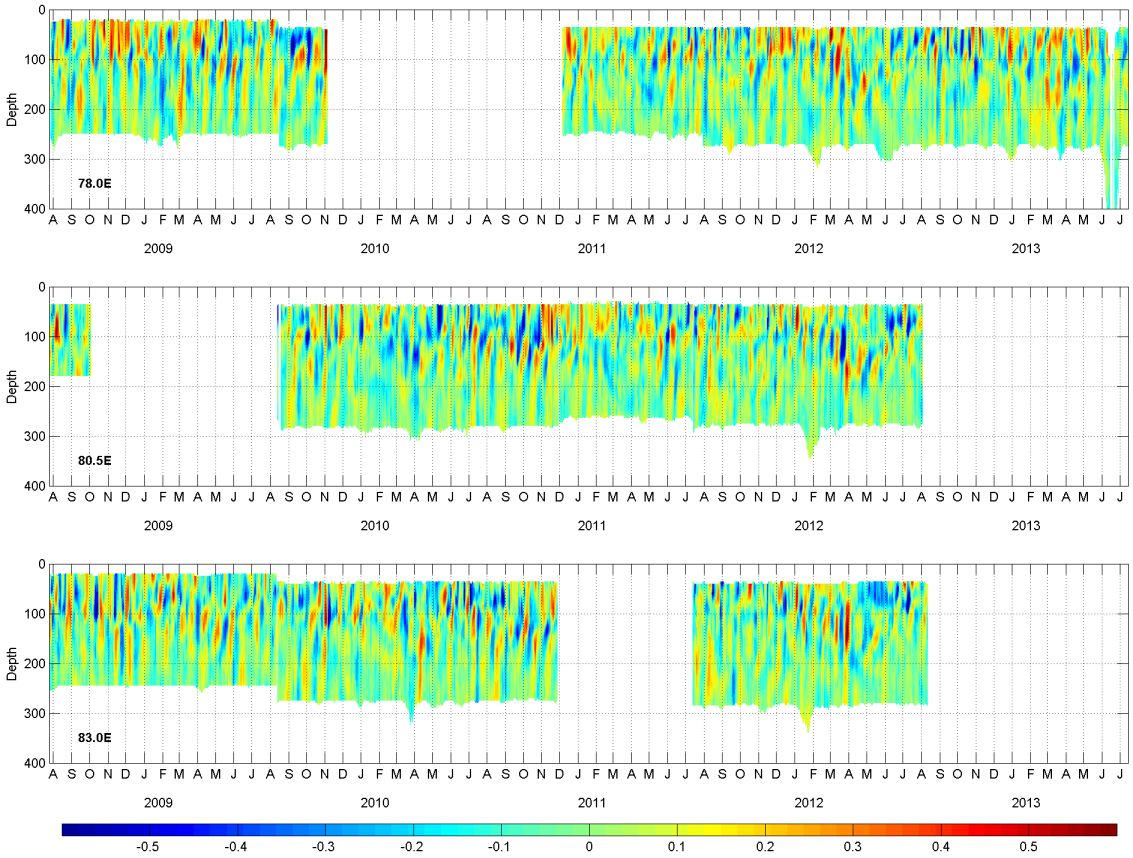

Figure 4b: The original dataset: Meridional velocity along the equator.

Table 1: ADCP mooring deployment information. Approximate depth of the ADCP head listed is based on the difference between estimated water depth and mooring length and represents the head depth when the mooring was completely vertical. Currents acting on the mooring may depress the ADCP depth. Time series of pressure near the head recorded by the ADCP and by two instruments on the buoy frame were used to calculate more accurate bin depths for each velocity profile.

Location	Time Interval	Deployment Depth of ADCP Head (m)
4.0°S, 80.5°E	19 August 2008 to 5 September 2009	333.5
	6 September 2009 to 16 June 2011	455.5
	18 December 2010 to 2 August 2011	299.5
2.5°S, 80.5°E	18 August 2008 to 17 December 2010	308.5
	17 December 2010 to 1 August 2011	301.5
1.5°S, 80.5°E	3 September 2009 to 16 December 2010	302.0
	16 December 2010 to 30 July 2011	297.5
	31 July 2011 to 22 August 2012	316.0
0.75°S, 80.5°E	15 August 2008 to 10 May 2010	300.5
	10 May 2010 to 18 June 2011	257.5
	18 June 2011 to 20 August 2012	292.9
0.0°, 80.5°E	9 August 2008 to 18 May 2009	299.9
	27 August 2009 to 14 December 2010	316.0
	14 December 2010 to 29 July 2011	297.5
	27 July 2011 to 18 August 2012	316.0
0.75°N, 80.5°E	14 August 2008 to 23 May 2010	315.6
	23 May 2010 to 11 July 2012	299.1
1.5°N, 80.5°E	12 August 2008 to 13 May 2009	302.9
	16 May 2009 to 8 May 2010	298.0
	8 May 2010 to 12 July 2012	284.5
2.5°N, 80.5°E	12 August 2008 to 20 September 2009	296.5
	20 September 2009 to 10 December 2010	315.5
	10 December 2010 to 15 August 2011	315.5
0.0°, 78.0°E	10 August 2008 to 29 August 2009	293.5
	29 August 2009 to 20 December 2010	319.0
	20 December 2010 to 13 August 2011	293.5
0.0°, 83.0°E	7 August 2008 to 26 August 2009	299.6
	26 August 2009 to 12 December 2010	324.0
	26 July 2011 to 26 August 2012	328.0

3. Processing to Continuous Time Series

Daily averaged current data were computed from the vertically gridded hourly data. Sequential deployments from the same sites were combined to form multi-year time series, from which 5-day running means were made to filter the high-frequency variability. The 1- or 2-day gaps between deployments were also filled by this smoothing. Five longer gaps were also filled via linear orthogonal regression to provide a continuous time series. The gridding and filling procedures are described below.

3.1 Gridding

In order to extend the data records to the surface, different strategies were adopted to extrapolate zonal and meridional velocities. Sontek records from 1.5°N, 0°, and 1.5°S along 80.5°E at 10 m depth were then used to evaluate the extrapolation. The values of the zonal velocity near the surface were directly replaced with the values at the shallowest depths available. This method worked well based on the high correlation between the moored ADCP data at 25–40 m and Sontek records at 10 m (**Figure 5**). The correlation coefficient for 5-day averages at 0°, 1.5°S, and 1.5°N along 80.5°E were 0.98, 0.93, and 0.94, respectively, while the slope of the orthogonal regression was close to 1.0 (0.97, 0.97, and 0.92, respectively).

The meridional velocities near the surface were extrapolated using a different strategy because of the high near-surface shear in this component. In particular, we used a quadratic spline extrapolation of the form $V_z = (aD_z + b)\,[V_{35} + (V_{30} - V_{35})\,(D_z - D_{35}) / (D_{30} - D_{35})]$ in the upper 30 m. In this equation, V indicates the meridional velocity and D indicates the depth. The subscript z indicates a target depth for extrapolation, while subscripts 30 and 35 indicate depths of 30 m and 35 m. The term in brackets, $V_{35} + (V_{30} - V_{35})\,(D_z - D_{35}) / (D_{30} - D_{35})$, represents a linear extrapolation. The term $aD_z + b$ is a gain factor chosen to make the variance of the interpolated record equal to that of the Sontek at 10 m, equal to the ADCP record at 30 m, and linearly varying between these two levels. The constraint at 30 m requires $30a + b = 1$, while the constraint at 10 m provides a second condition to determine a and b. For profiles where valid values of velocity start from 40 m or deeper, a linear extrapolation from the shallowest two values was first made to get V_{30} and V_{35}, after which the equation for V_z was applied. The extrapolation strategy was evaluated by orthogonal regression between the values of Sontek records and the extrapolation at 10 m. Results presented in **Figure 6** show good correspondence between observed (from Sontek) and estimated (from the extrapolation) meridional velocities at 10 m depth, with correlation coefficients of 0.85, 0.86, and 0.72 and slopes of the orthogonal regression of 0.85, 0.98, and 1.1, respectively at 0°, 1.5°S, and 1.5°N along 80.5°E. We do not have Sontek data to verify the extrapolation at sites other than these three sites, so meridional velocities shallower than 35 m should be interpreted with caution at other locations.

3.2 Filling gaps

Five main gaps occurred in the original time series (**Table 2**). These gaps were filled via linear regression using formulae of the form $X_{\text{estimate}} = aX_1 + bX_2 + c$ where X is either zonal or meridional velocity. X_1 and X_2 indicated the value of the velocity at adjacent sites, while the coefficients a, b, and c were determined by linear least squares orthogonal regression. The method is similar to that used by McPhaden and McCarty (1992) and Johnson and McPhaden (1993) to fill gaps in velocity time series from the equatorial Pacific Ocean. Along the 80.5°E section, the gap during August 2008 to September 2009 at 0° was filled by the records from same time period at 0.75°N and 0.75°S, the gap during August 2008 to September 2009 at 1.5°S was filled by the records from same time period at the sites 0.75°S and 2.5°S, and the gap during September–December 2010 at 2.5°S was filled by the records from same time period at 1.5°S and 4.0°S. Along the equator, because there were only three sites, the coefficient b was set to zero so that only the time series from same period at 80.5°E were used to fill the gaps during November 2009 to December 2010 at 78.0°E and December 2010 to July 2011 at 83.0°E.

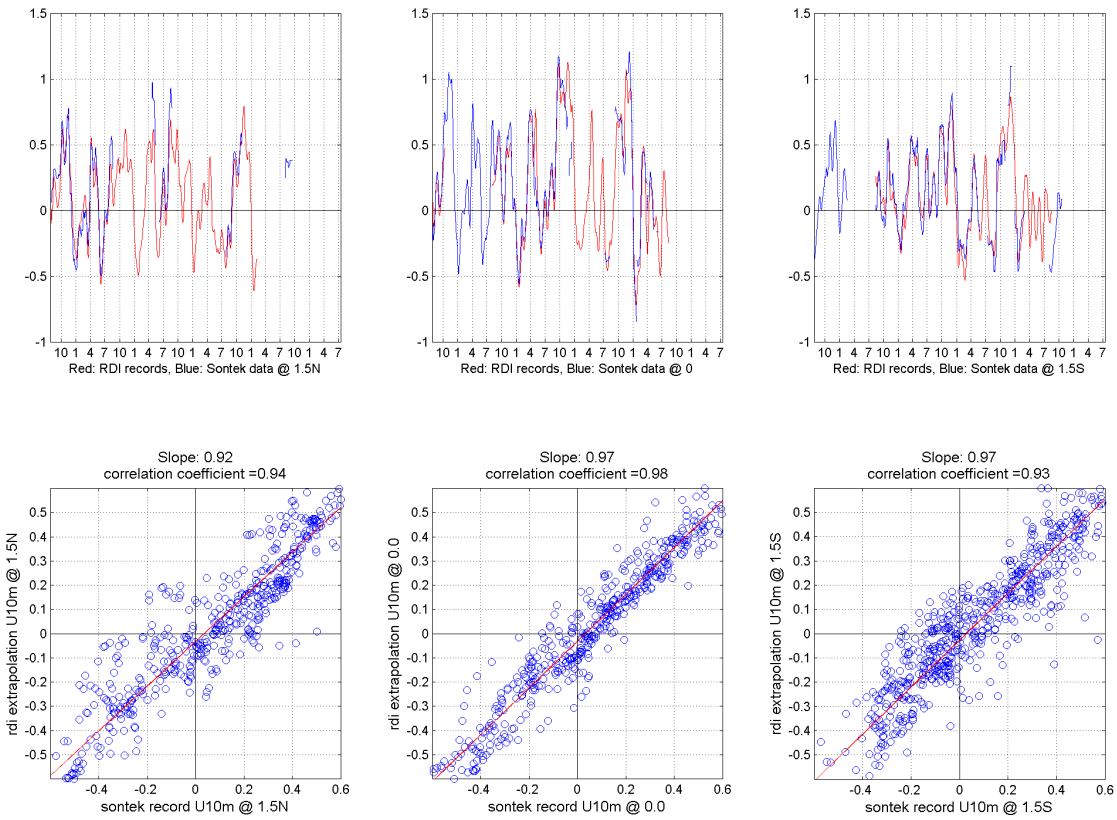

Figure 5: Correlation and regression between zonal velocity extrapolated to 10 m from the moored ADCP data and zonal velocity at 10 m from Sontek records. To better illustrate correspondence between the actual and extrapolated currents, time series in the upper panel were smoothed with a 15-day running mean.

The filled time series are presented in **Figures 7** and **8**. The translucent overlay of the time series indicates records calculated by extrapolation or linear regression. Due to the weak correlation of the meridional velocity between sites in the zonal direction (presented in Section 4.2), the meridional time series along the equator were not filled.

Table 2: Gaps in the time series of the ADCP data.

	Location	Gap Interval
1	0°, 80.5°E	18 October 2008 to 1 September 2009
2	1.5°S, 80.5°E	8 August 2008 to 3 September 2009
3	2.5°S, 80.5°E	1 September 2010 to 17 December 2010
4	0°, 78.0°E	20 November 2009 to 19 December 2010
5	0°, 83.0°E	12 December 2010 to 26 July 2011

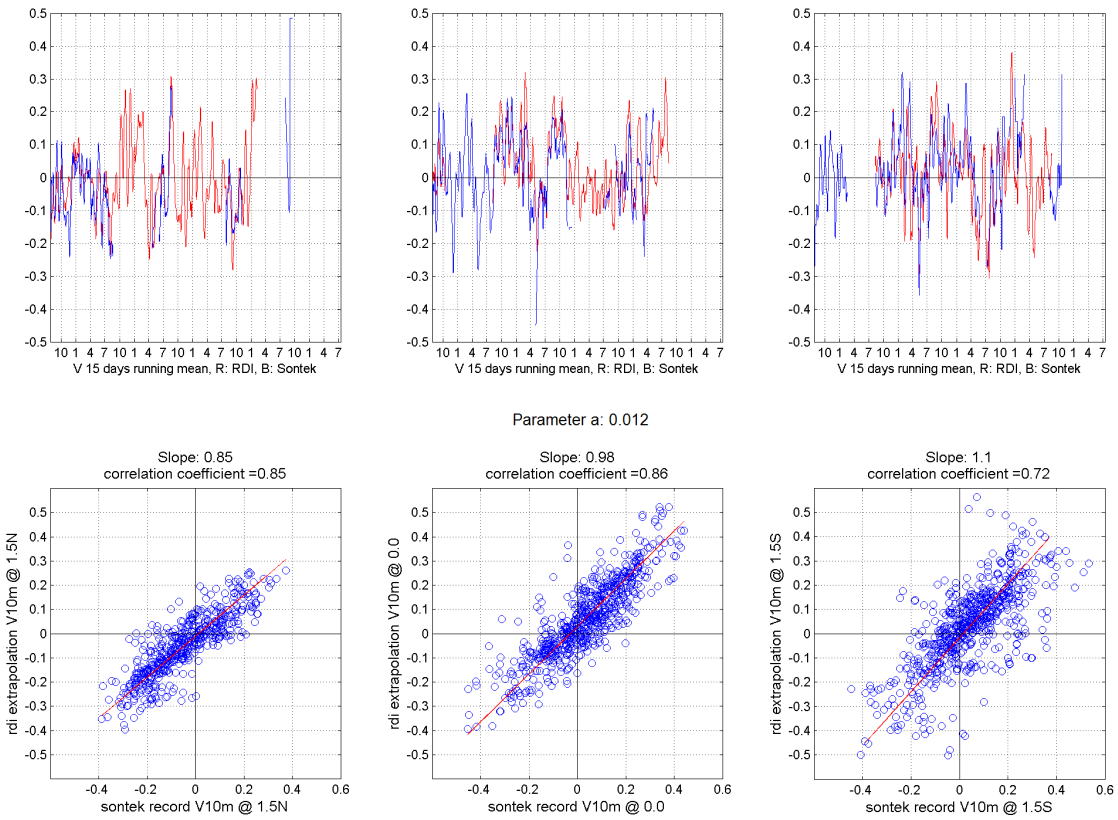

Figure 6: Correlation and regression between the extrapolated meridional velocity at 10 m depth from moored ADCP data and the meridional velocity at 10 m from Sontek records. To better illustrate correspondence between the actual and extrapolated currents, time series in the upper panel were smoothed with a 15-day running mean.

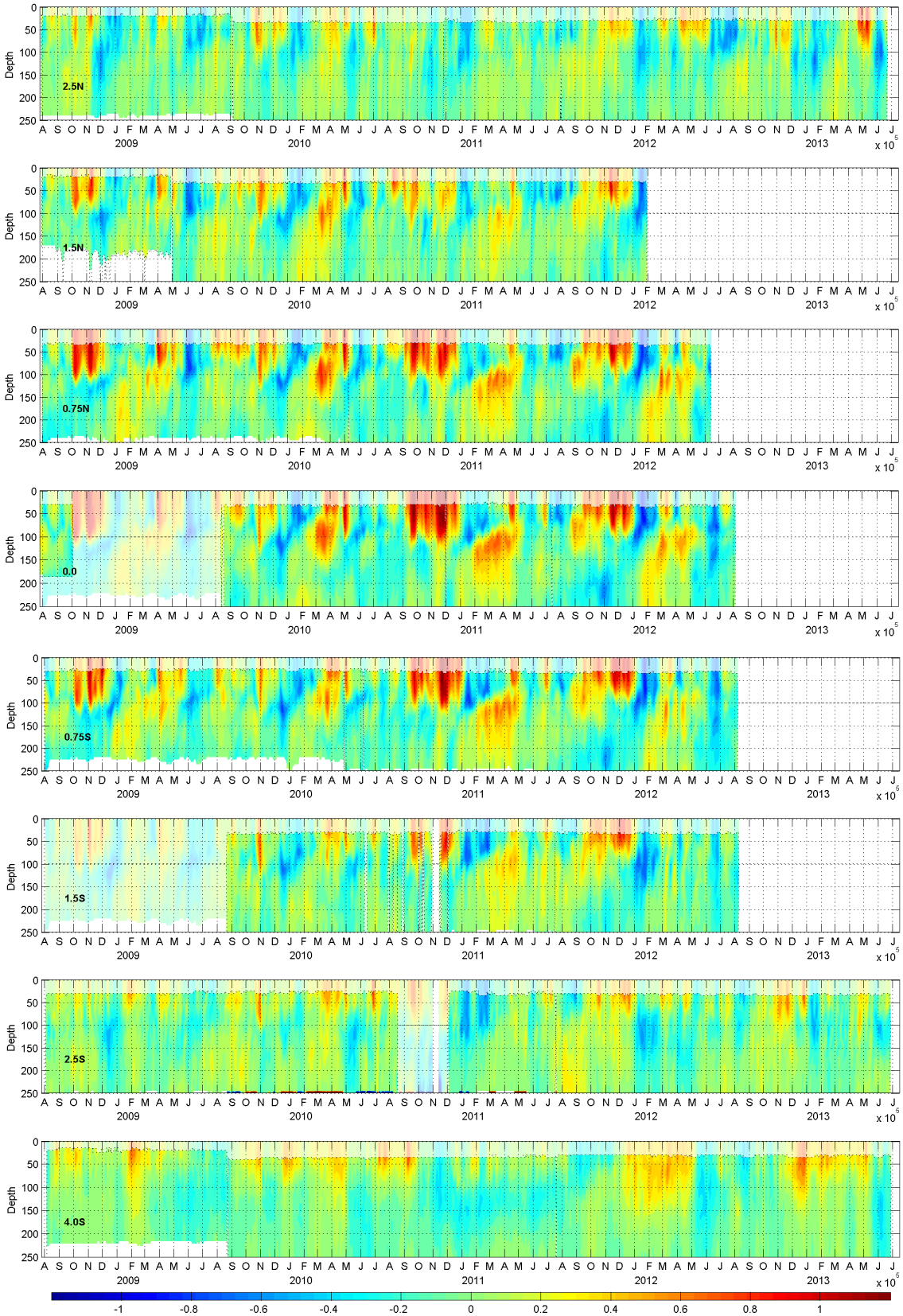

Figure 7a: The filled zonal velocity time series along the 80.5°E meridional section.

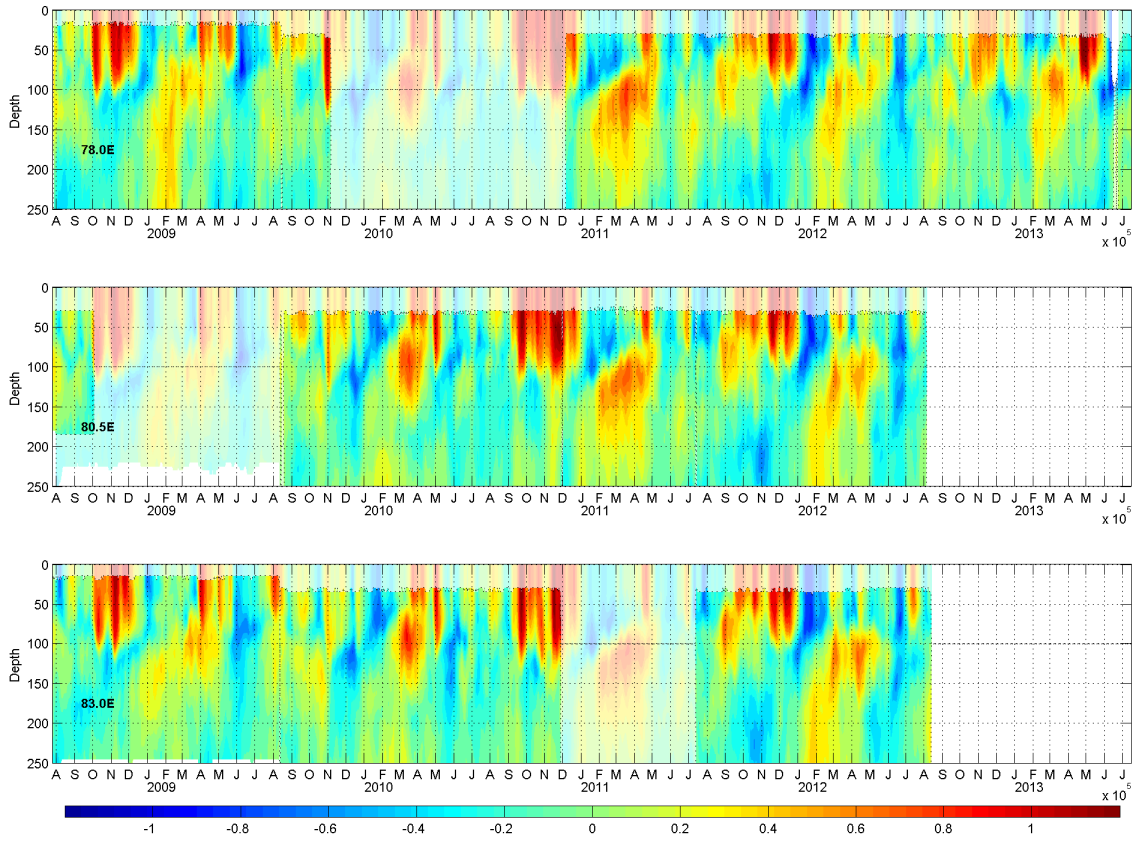

Figure 7b: The filled zonal velocity time series along the equator.

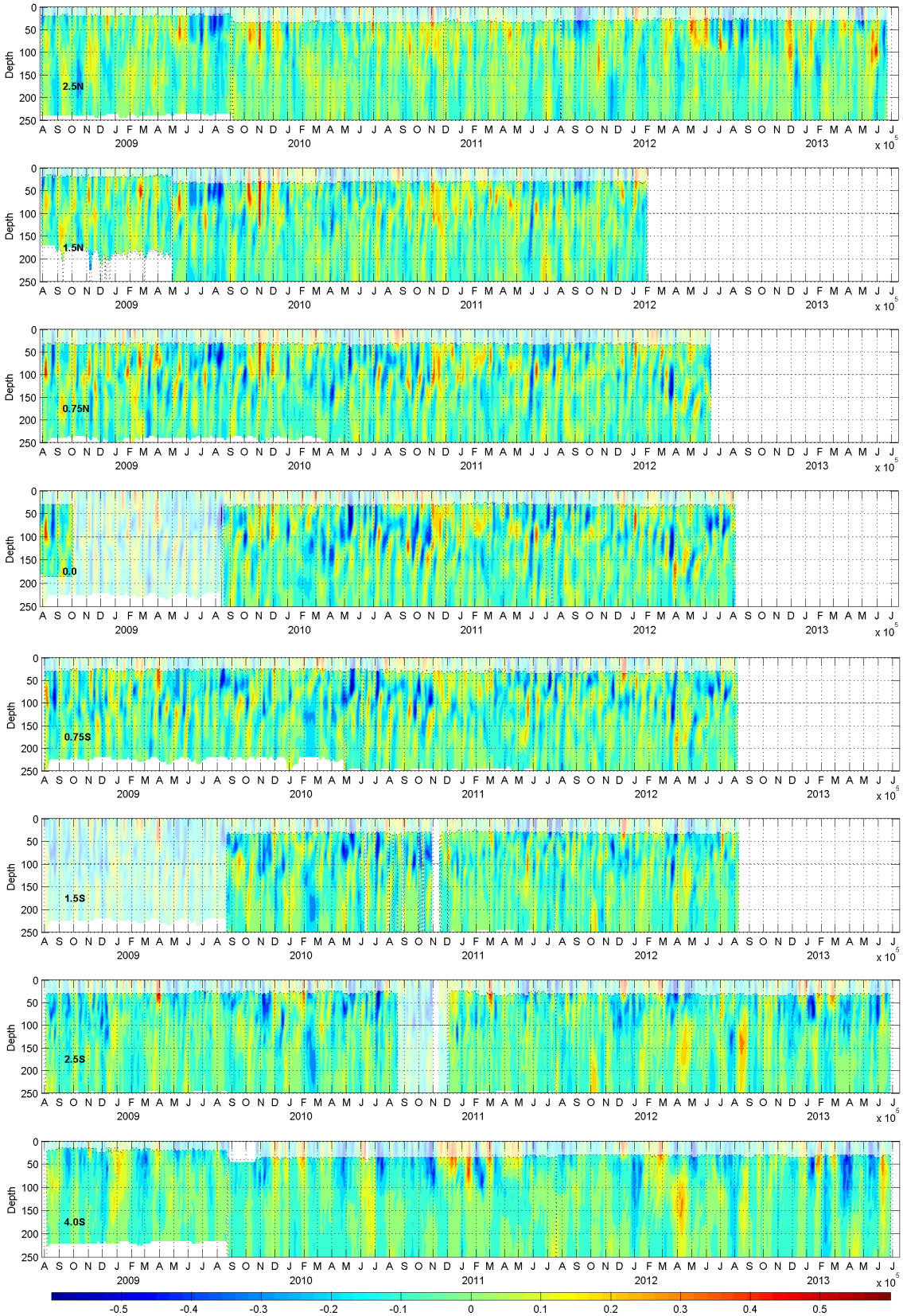

Figure 8: The filled meridional velocity time series along the 80.5°E meridional section.

4. Evaluation of the Filled Time Series

4.1 Evaluating the regression strategy for filling gaps

We filled the gap at 0.75°N, 80.5°E from May 2010 to July 2011 before the ADCP mooring for this period was recovered but while the records at 0.75°S, 80.5°E and 0°, 80.5°E were available. Hence, this time interval at 0.75°N, 80.5°E was regarded as a long gap and filled by extrapolation. When the mooring at 0.75°N, 80.5°E was eventually recovered and the data after May 2010 made available, we compared the actual velocity and the prior regression fill to evaluate our regression strategy.

Figures 9 and **10** compare the time series of the actual velocity and the regression fill. The patterns are similar at depths shallower than 200 m. At deeper depths, the regression fill becomes noisy, especially for meridional velocity. Scatter plots (**Figure 11**) of all velocity values shallower than 200 m show correlation coefficients between actual zonal (meridional) velocity and regression fill zonal (meridional) velocity reaches of 0.91 (0.83). Based on these high correlations and the regression slopes, which are close to 1, our method appears to work very well for filling gaps shallower than 200 m.

4.2 Metrics for evaluating regression fills

We used the regression formula to estimate velocities at times when there were no gaps in order to evaluate the expected errors in the estimated velocity X_{estimate} when there were gaps. Expected errors were determined by computing the correlation between X_{estimate} and the actual velocity X, root-mean-square (RMS) deviations, and normalized RMS deviations, i.e., $RMSD = RMS\ (X_{\text{estimate}} - X)$ and $NRMSD = RMSD / STD\ (X)$. The RMSD of the zonal and meridional velocity at the five sites were 0.05–0.2 m s^{-1} at depths between 20 m and 200 m. It can be inferred that the combined errors from the extrapolation to the surface and the linear regression increase the RMSD near the surface for meridional velocity.

The correlation coefficients for zonal velocity exceeded 0.8 at almost every depth level at most sites, though they were lower farther from the equator along 80.5°E. At 2.5°S, 80.5°E, the coefficients were 0.65–0.75 at 100–200 m depths while at 0°, 80.5°E, the coefficients exceeded 0.95 at every depth (**Figure 12**). Because meridional velocity is weaker relative to zonal velocity, the correlation coefficients for meridional velocity are about 0.1 lower than the zonal velocity above 200 m. The method of using regression analysis to fill gaps in meridional velocity along the equator was unsuccessful because of longer distance between sites and presumably the shorter zonal coherence scales for meridional velocity. Correlation coefficients in this case were 0.5 or lower, so we chose to leave the meridional velocity gaps at 78.0°E and 83.0°E unfilled.

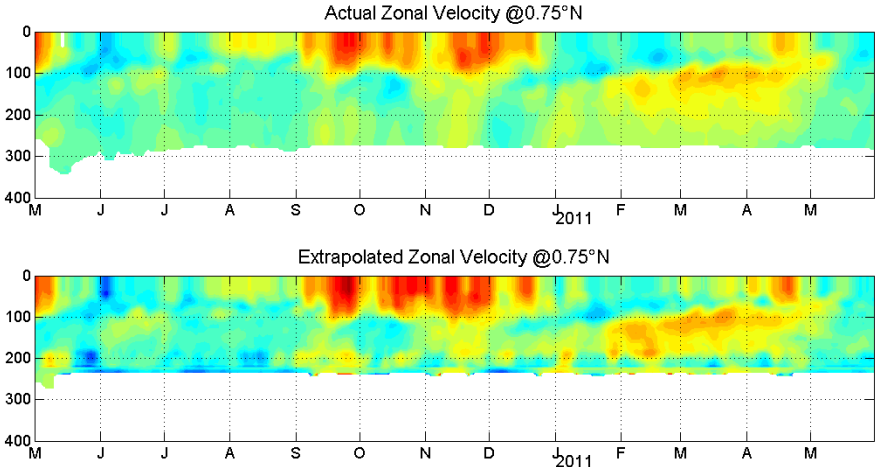

Figure 9: The actual and extrapolated zonal velocity at 0.75°N, 80.5°E.

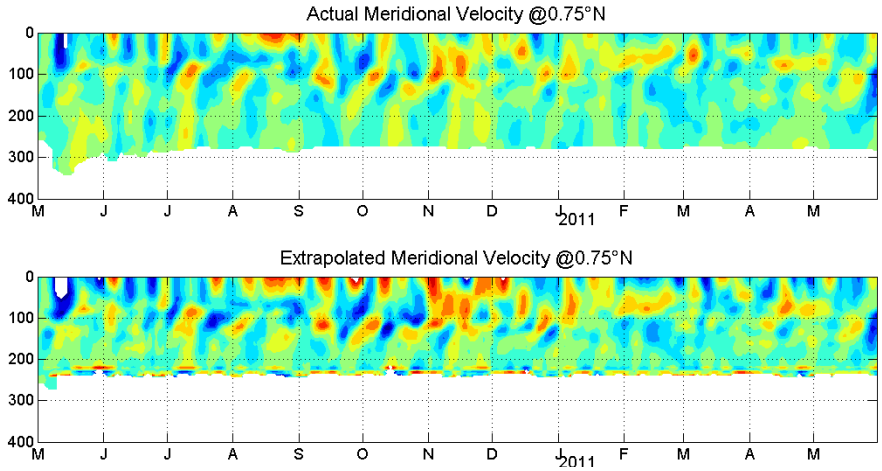

Figure 10: The actual and extrapolated meridional velocity at 0.75°N, 80.5°E.

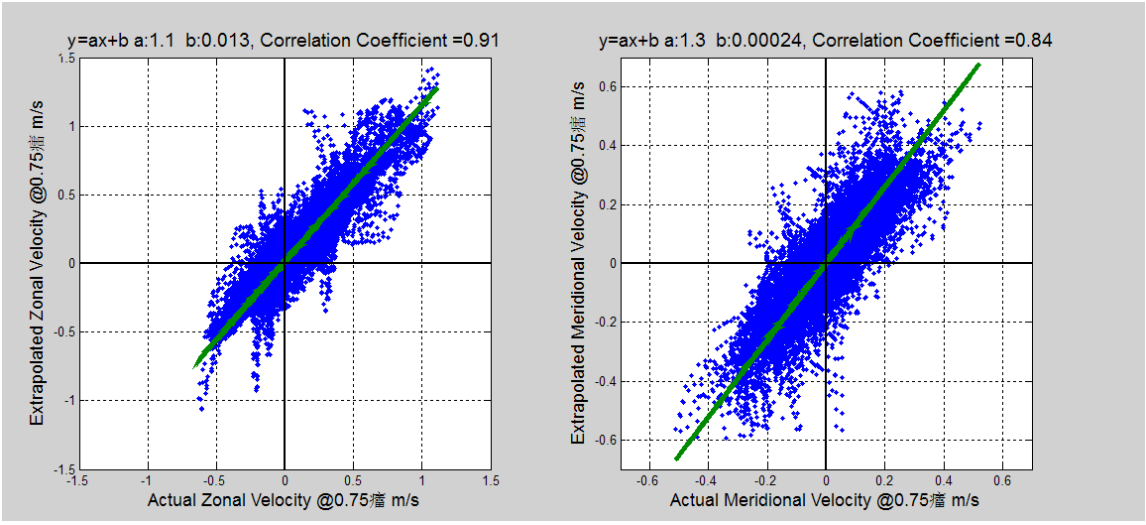

Figure 11: Scatter plots of all velocity values shallower than 200 m between actual and extrapolated velocity.

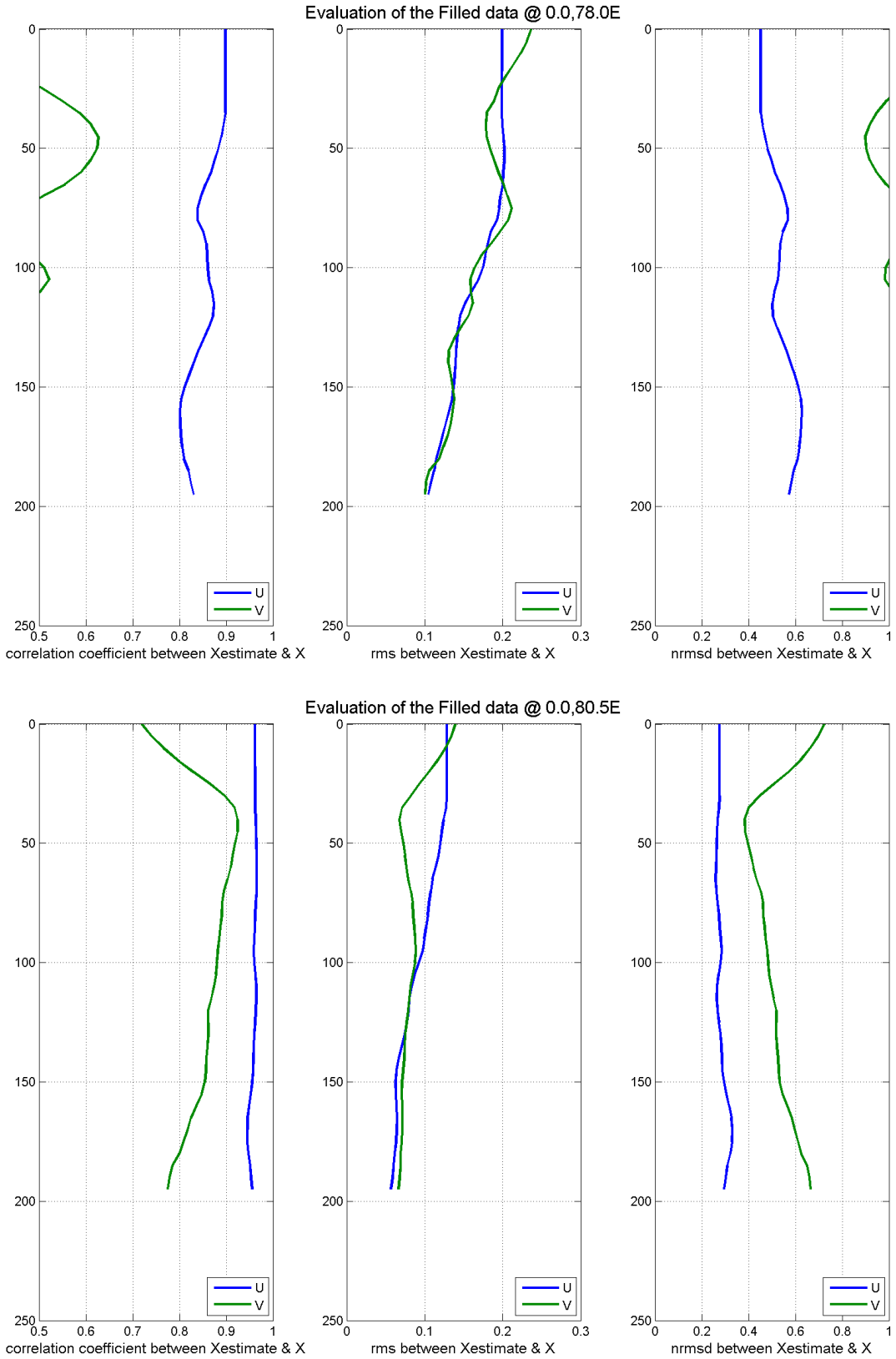

Figure 12: Metrics for estimated velocity at (a) 0°, 78°E and (b) 0°, 80.5°E.

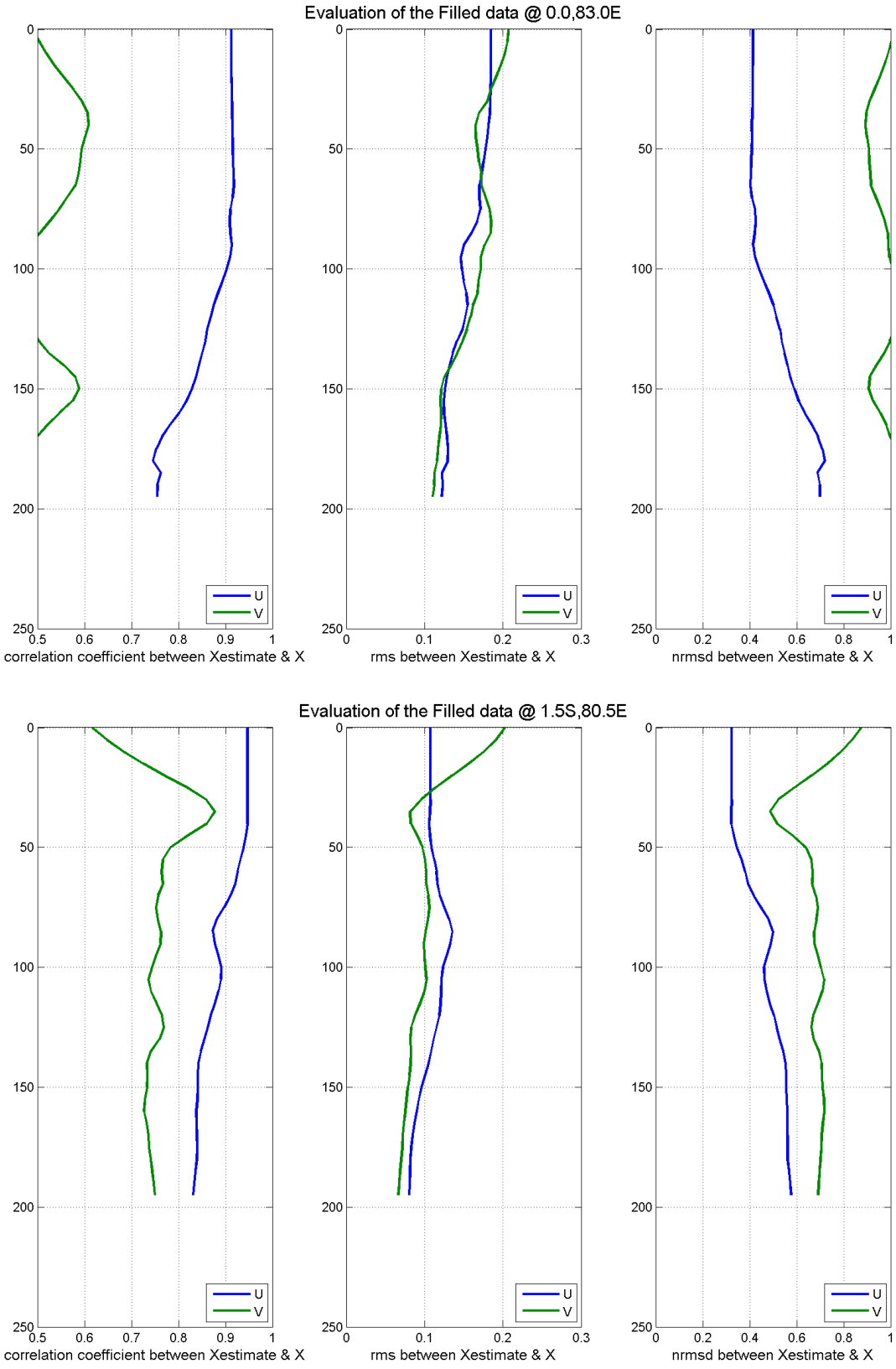

Figure 12, continued: Metrics for estimated velocity at (c) 0°, 83°E and (d) 1.5°S, 80.5°E.

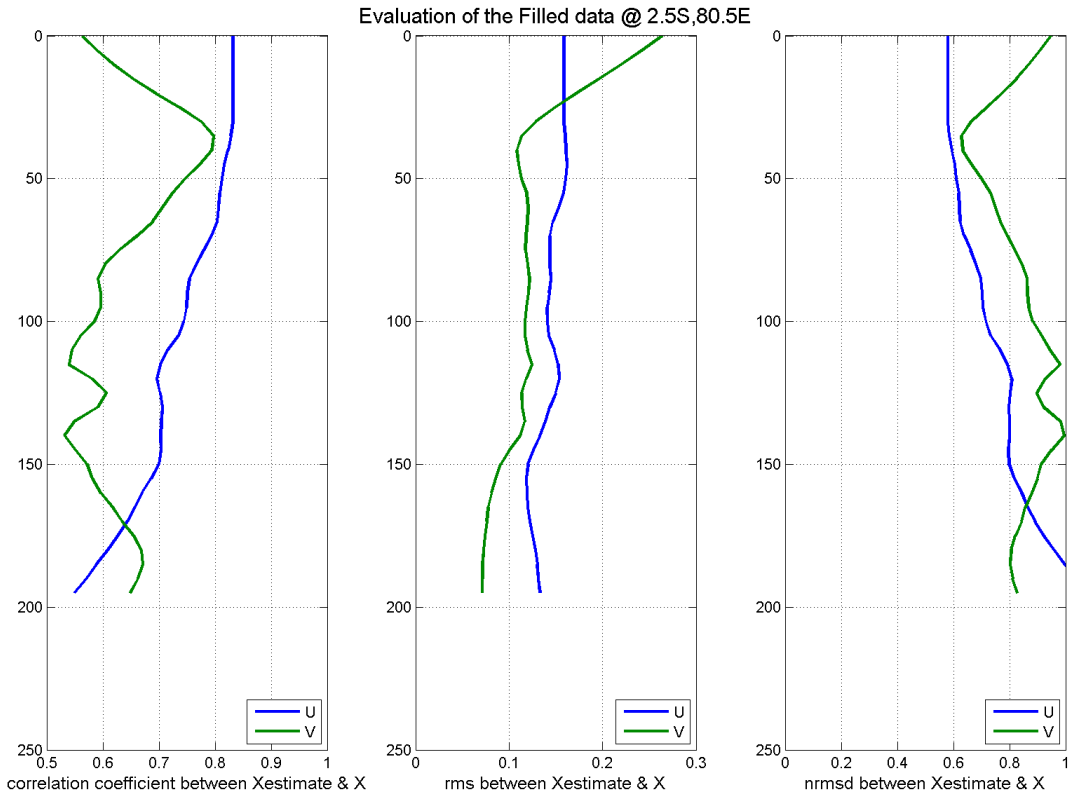

Figure 12, continued: Metrics for estimated velocity at (e) 2.5°S, 80.5°E.

5. Acknowledgments

This work was carried out while Wang Yi visited the Pacific Marine Environmental Laboratory from the Ocean University of China. The work was supported by NOAA and by the Joint Institute for the Study of the Ocean and Atmosphere at the University of Washington in Seattle. This publication is partially funded by the Joint Institute for the Study of the Atmosphere and Ocean (JISAO) under NOAA Cooperative Agreement No. NA10OAR4320148. PMEL contribution number 4307 and JISAO contribution number 2427.

6. References

Gnanaseelan, C., A. Deshpande, and M.J. McPhaden (2012): Impact of Indian Ocean Dipole and El Niño/Southern Oscillation forcing on the Wyrtki jets. *J. Geophys. Res., 117*, C08005, doi:10.1029/2012JC007918.

Iskandar, I., and M.J. McPhaden (2011): Dynamics of wind-forced intraseasonal zonal current variations in the equatorial Indian Ocean. *J. Geophys. Res., 116*, C06019, doi:10.1029/2010JC006864.

Johnson, E.S. and M.J. McPhaden (1993): On the structure of intraseasonal Kelvin waves in the equatorial Pacific Ocean. *J. Phys. Oceanogr., 23*, 608–625.

Masumoto, Y., T. Horii, I. Ueki, H. Hase, K. Ando, and K. Mizuno (2008): Short-term upper-ocean variability in the central equatorial Indian Ocean during 2006 Indian Ocean Dipole event. *Geophys. Res. Lett., 35*, L14S09, doi:10.1029/2008GL033834.

McPhaden, M.J., *et al.* (2009): RAMA: The Research Moored Array for African–Asian–Australian Monsoon Analysis and Prediction. B*ull. Am. Meteorol. Soc., 90*, 459–480, doi:10.1175/2008BAMS2608.1.

McPhaden, M.J., and M.E. McCarty (1992): Mean seasonal cycles and interannual variations at 0°, 110°W and 0°, 140°W during 1980–1991. *NOAA Tech. Memo. ERL PMEL-95*, NOAA/Pacific Marine Environmental Laboratory, Seattle, WA, 64 pp.

Nagura, M., and M.J. McPhaden (2008): The dynamics of zonal current variations in the central equatorial Indian Ocean. *Geophys. Res. Lett., 35*, L23603, doi:10.1029/2008GL035961.

Nagura, M., and M.J. McPhaden (2010a): Wyrtki jet dynamics: Seasonal variability. *J. Geophys. Res., 115*, C07009, doi:10.1029/2009JC005922.

Nagura, M., and M.J. McPhaden (2010b): Dynamics of zonal current variations associated with the Indian Ocean dipole. J. *Geophys. Res., 115*, C11026, doi:10.1029/2010JC006423.

Plimpton, P.E., H.P. Freitag, and M.J. McPhaden (2004): Processing of subsurface ADCP data in the equatorial Pacific. *NOAA Tech. Memo. OAR PMEL-125*, NOAA/Pacific Marine Environmental Laboratory, Seattle, WA, 41 pp.

Saji, N.H., B.N. Goswami, P.N. Vinayachandran, and T. Yamagata (1999): A dipole mode in the tropical Indian Ocean. *Nature, 401*, 360–363.

Wyrtki, K. (1973): An equatorial jet in the Indian Ocean. *Science, 181*(4096), 262–264, doi:10.1126/science.181.4096.262.